ISSN 0005-1055, Automatic Documentation and Mathematical Linguistics, 2025, Vol. 59, Suppl. 2, pp. S152–S159. © Allerton Press, Inc., 2025.
Russian Text © The Author(s), 2025, published in Elektronnye Biblioteki, 2025, Vol. 28, No. 2, pp. 378–397.

New Possibilities of the Fourier Transformation: How to Describe an Arbitrary Frequency-Phase Modulated Signal?

R. R. Nigmatullin[a], * (ORCID: 0000-0003-2931-4428), A. A. Litvinov[a], ** (ORCID: 0009-0000-3901-3704), and S. I. Osokin[b], * (ORCID: 0000-0002-0699-5390)**

[a] *Kazan National Research Technical University named after A.N. Tupolev, Radioelectronics and Informative Measurements Technics department, Kazan, 420111 Russia*

[b] *Kazan Federal University, Institute of Information Technologies and Intellectual Systems, Kazan, 420008 Russia*

**e-mail: renigmat@gmail.com,*

***e-mail: litvinov85@gmail.com*

****e-mail: s.osokin@it.kfu.ru*

Received February 14, 2025

Abstract—In this paper, the authors identify a transformation that is valid for any *arbitrary* signal. This transformation is strictly periodical and therefore it allows the ordinary F-transformation to be applied for the fitting of the transformed signal. The most interesting application (in accordance with the authors' opinion) is the fitting of the frequency-phase modulated signals that actually located inside the found transformation. This new transformation will be useful for the application of the responses of different complex systems when an ordinary model is absent. As available information we consider meteorological data corresponding to measurements of methane concentration (CH_4) in atmosphere during 4 weeks of observation. For us, it is important to consider the integral (cumulative) data and find their amplitude-frequency response (AFR). If one considers each column as a frequency-phase modulated signal, then the AFR can be evaluated with the help of an F-transformation with a period equaling 2π that is valid for any analyzed random signal. This "universal" F-transformation allows us to fit a wide set of random signals and compare them with each other in terms of their AFRs. In conclusion, these new possibilities of traditional F-analysis will serve as a common tool in the armory of the methods used by researchers in data processing area.

Keywords: Fourier transform, random signal, frequency-phase modulated signal, amplitude-frequency response, complex systems, meteorological data, eddy covariance

DOI: 10.3103/S0005105525700761

1. INTRODUCTION AND STATEMENT OF THE PROBLEM

Everyone knows the main drawback of the traditional Fourier transform. It consists of the assumption that any digital random signal is periodic, i.e.,

$$\mathrm{Sg}(t + T) = \mathrm{Sg}(t). \quad (1)$$

Here, $\mathrm{Sg}(t)$ is an arbitrary random signal, and T is the period coinciding with Range(t). $\mathrm{Range}(t) = \max t - \min t$ determines the length of the analyzed signal $\mathrm{Sg}(t)$. In many cases, this assumption concerning the periodicity of the signal is unprovable, but is still used.

If we want to replace a purely periodic signal with its aperiodic copy, the problem of the impossibility of approximating a discrete aperiodic signal arises. This problem cannot be solved with the integral Fourier transform of aperiodic signals, therefore, it cannot be used to predict the aperiodic signal outside of the given time window interval.

Discrete representations of many analog signals play an important role in their processing. They contain necessary information related to the properties of signals and allow their further processing [1]. In the traditional scheme, signals can be represented as Taylor-Maclaurin, Dirichlet, Laurent, Legendre, Padé, Prony, and Fourier series. We emphasize that, in our opinion, these expansion series can be used to describe data without any mathematical justification. In signal processing, the classical Fourier series is a simple, frequently used tool. However, it does not allow us to isolate both the subharmonic and the interharmonic components of a given signal, and in many situations, it has serious drawbacks [2–5]. The proposed method allows the limitations of Fourier analysis to be overcome. Fourier analysis is based on time-frequency methods [6] that have been used in recent decades, namely, discrete [7–9], fast [10–12], windowed Fourier transform [13, 14], Gabor transform [15–17], wavelet [18–20], Hilbert–Huang transform [21–23], Fourier–Bessel transform [24, 25], and even empirical

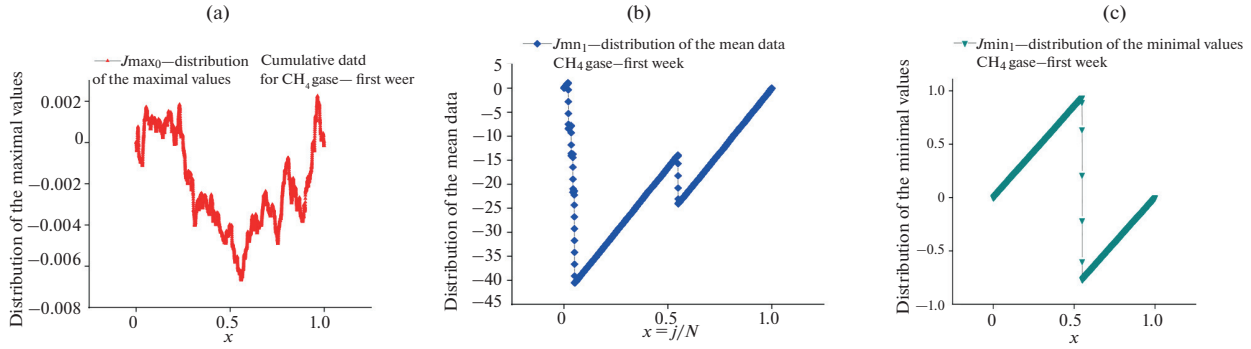

Fig. 1. The left panel shows the curve with the maximum values, the center gives the average data (averaged over the entire measurement period), and on the right is the curve with the minimum values.

mode decomposition [26, 27]. The cited works indicate that there are many different approximations that can be used to overcome the main drawback (1) that is associated with the periodicity assumption. However, a careful analysis of these approximations allows us to formulate the following problem: determining whether there is a universal transformation of the original signal that allows it to be transformed into another digital signal with a period of exactly 2π. Indeed, if we write the following relationship:

$$\mathrm{Sg}(t) = a\cos(F(t)) + b \qquad (2)$$

and begin to analyze the argument F(t) of the cosine in (2) instead of the original function Sg(t), we get the desired result. The function $F(t)$ is a combined frequency-phase modulated signal, providing the desired interval $[-1, 1]$ for cos(F(t)), and the argument $F(t)$ falls in the interval $[0, \pi]$. Therefore, the final result of the decomposition of any signal $\cos(\Omega_k t)$ retains the previous form (2) if we add to it the expansion of $F(t)$ by the approximating function $Yft(t, \mathrm{K})$ in the form of a finite segment of the Fourier series

$$F(t) \cong Yft(t, K)$$
$$= Ph_0 + \sum_{k=1}^{K}\left[Ac_k \cos(\Omega_k t) + As_k \sin(\Omega_k t)\right], \qquad (3)$$
$$\Omega_k = 2, 3, \ldots, K.$$

Here, we take into account the property $F(t) = F(t \pm \pi)$, which defines a semi-periodic function. Thus, these two simple expressions (2) and (3) quite effectively solve the problem of decomposing any random function Sg(t) into a Fourier series, as in this case, the problem of the periodicity of the signal being decomposed is solved.

2. DESCRIPTION OF WEATHER DATA

Let us say a few words about the real data and its features. As real data, we took the eddy covariance environmental data related to the methane content CH_4 in the atmosphere. In this paper we consider the methane balance, i.e., the product of the corresponding concentration and the value of the vertical velocity. Data were taken from instruments on a tower located near the Kazan University Observatory; these instruments measured eddy covariances associated with the methane content in the atmosphere and air flow speeds. The measurements of methane concentration CH_4 (μmol/mol) and vertical air velocity W (m/s) were carried out from January 1 to January 7, 2024. CH_4 data values were multiplied by the corresponding measured values of air flow velocity W. The measurement frequency was 10 times per second. The data for 1 second was averaged, and the second-long (averaged) values were collected into hourly groups/columns. The result was 168 hourly columns per week with 3600 seconds per column.

3. DESCRIPTION OF THE PROCESSING PROCEDURE

Each rectangular matrix N × M contains N = 3600 rows (where each row corresponds to 1 second of measurements and, therefore, one column corresponds to 1 hour of measurements), and the number of columns M = 24×7 = 168 corresponds to 1 week of measurements. In demonstrating a new modification of the Fourier transform, we only consider three base curves corresponding to the maximum, average and minimum values. These curves are shown in Fig. 1, with independent variable $x_j = j/N$ ($N = 3600$). We normalized the independent variable to the total number of measurements in one hour.

Calculation of the arguments $Fq(t)$ ($q = 0, 1, 2$) from (2) for these curves located in the interval $(0, \pi)$, as shown in Fig. 2.

To find the AFR for these three curves, it is convenient to use the NOCFASS (Non-Orthogonal Combined Fourier Analysis of the Smoothed Signals) method [28], proposed by one of the authors (RRN) of this work. The basic idea of the NOCFASS approach is to shift the extremal curve to the center of

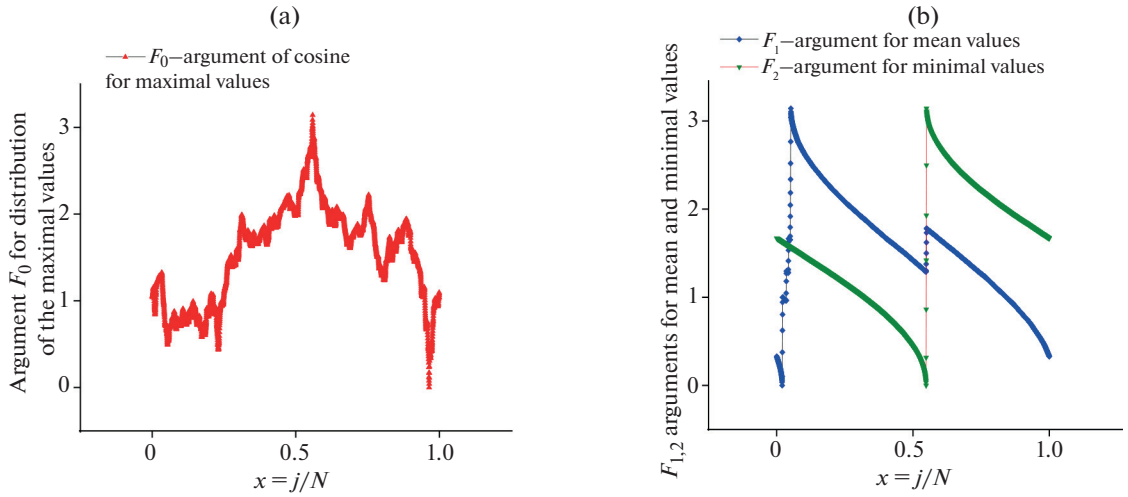

Fig. 2. The argument F is shown in the left panel, the $F_0(t)$ cosine functions in (2) for the maximum curve, and in the right panel are the corresponding arguments for the average curve $F_1(t)$ (blue dots) and the minimum curve $F_2(t)$ (green dots).

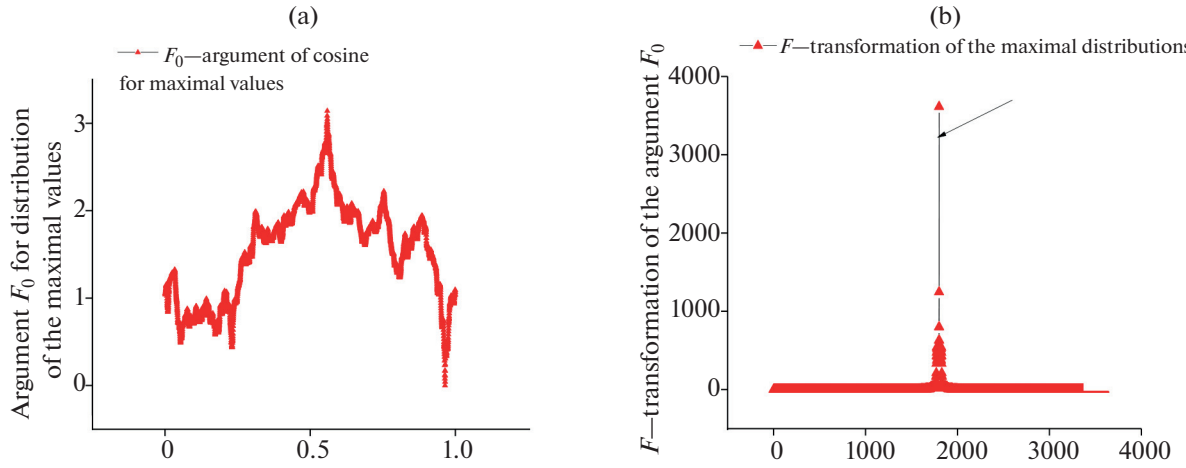

Fig. 3. The argument F is shown in the left panel, $F_0(t)$, corresponding to the curve with maximum values. In the right pane, is the Fourier transform shifted to the center $N/2 = 1800$, with a resonance value of 4032.668.

the Fourier transform using an angle π. It is demonstrated in Fig. 3.

Analysis of this Fourier transform showed that it is sufficient to take a small number of frequencies that are located in the vicinity of the resonant peak shown on the right. Therefore, we consider a dimensionless frequency band in the interval [1800, 2000].

This modified approach allowed us to reduce the number of modes, which significantly depends on the value of the final mode K. This value is determined by the magnitude of the relative error, which, in turn, is calculated as

$$\mathrm{RelErr}(K) = \left[\frac{\mathrm{stdev}(F(t) - Yft(t,K))}{\mathrm{mean}\,|F(t)|}\right] \times 100\%. \quad (4)$$

As an approximation, it is sufficient to take a small number of frequencies covering the interval [Vect, Vect + 200]. The final result is shown in Figs. 4 and 5.

The truncated spectrum shown in Fig. 4(a) is sufficient to provide an approximation with a relative error (defined by expression (4)) of less than 1%. The exact values of the relative error are collected in Table 1.

The AFR for the truncated spectrum is shown in Fig. 5.

The solid straight line shown on the right panel of the figure corresponds to the sequence of ranked amplitudes (SRA) of ordered phases. It is easy to see that the SRA is close in appearance to a straight line segment. This indicates that the phase distribution is almost uniform. To complete the approximation procedure, we demonstrate the transition from the

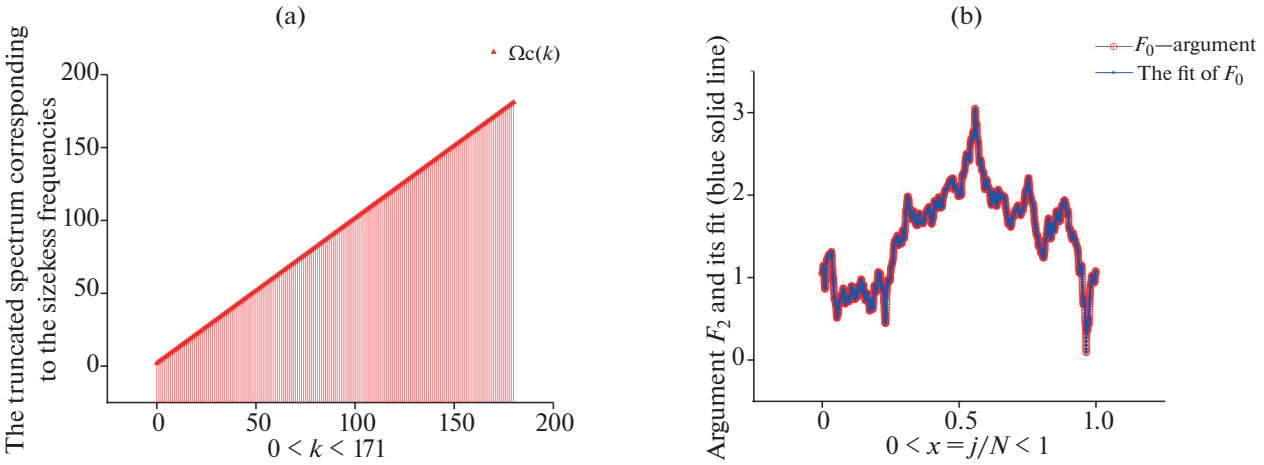

Fig. 4. In the left panel is shown a truncated spectrum located in the interval [2, 171]. In the right panel is the approximating function *Yft*(*t*) for the function $F_0(t)$.

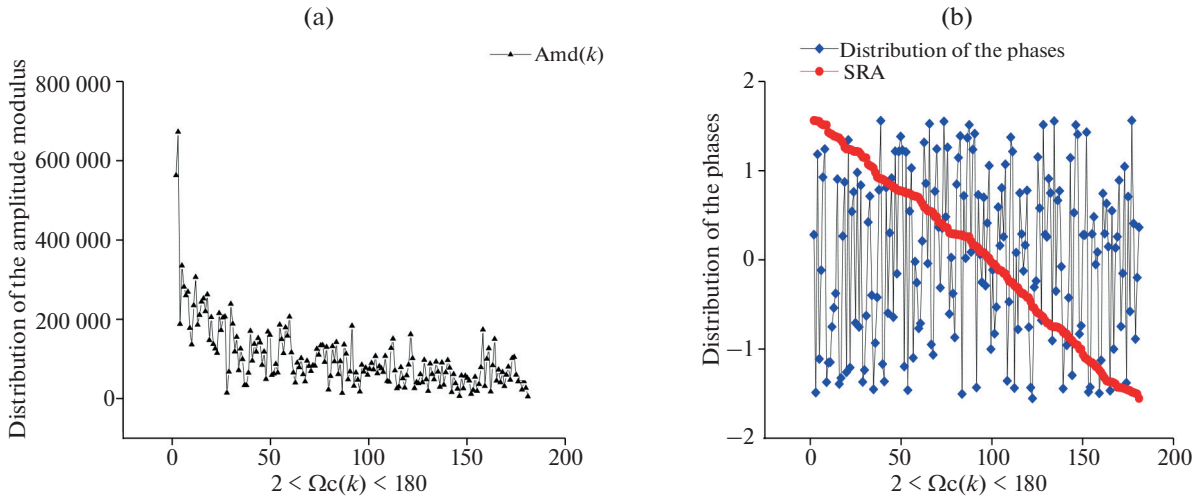

Fig. 5. The amplitude module is shown in the left, $\text{Amd}_k = \sqrt{\text{Ac}_k^2 + \text{As}_k^2}$, and in the right panel is the phase distribution $\text{Phase}_k = \tan^{-1}(\text{As}_k / \text{Ac}_k)$.

approximation of the argument $F_0(t)$ to the original signal Mex $(t)_0$ (see Fig. 6).

Figure 6 shows the restoration of the original signal. On the left you can see the scaled mex function$_0(t) = \cos(F_0(t))$ (red dots) and its approximation $\text{Jex}_0(Yft(t))$, shown by the blue solid line. To find the scaling parameters, the central figure can be used, which helps determine the slope ($a = 0.00446$) and intercept ($b = -0.00221$) values. The final approximating function is shown in the right figure as a blue solid line.

Table 1. The main parameters that were used to approximate the F functions$_p(t)$ ($p = 0.1.2$), corresponding to the first week of measurements

Function	Fres	Ph0	RelErr, %	*K*	*a*	*b*
*F*0(*t*)	4032.6694	0.0947	0.107	180	0.00446	–0.00221
*F*1(*t*)	3901.1394	0.0825	0.079	180	3.3585	3.8223
*F*2(*t*)	3571.141	0.9045	0.144	180	0.8517	0.0839

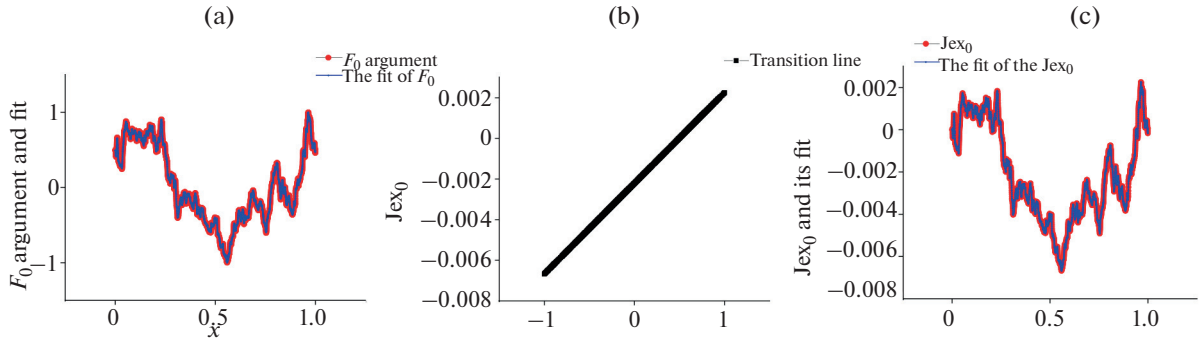

Fig. 6. The scaled mex function is shown in the left panel, $F_0(t) = \cos(F_0(t))$, along with its approximation $\mathrm{Jex}_0(Yft(t))$. The central panel helps to determine the values of the slope a and intercept b. In the right panel, the final fitting function is shown as a blue solid line.

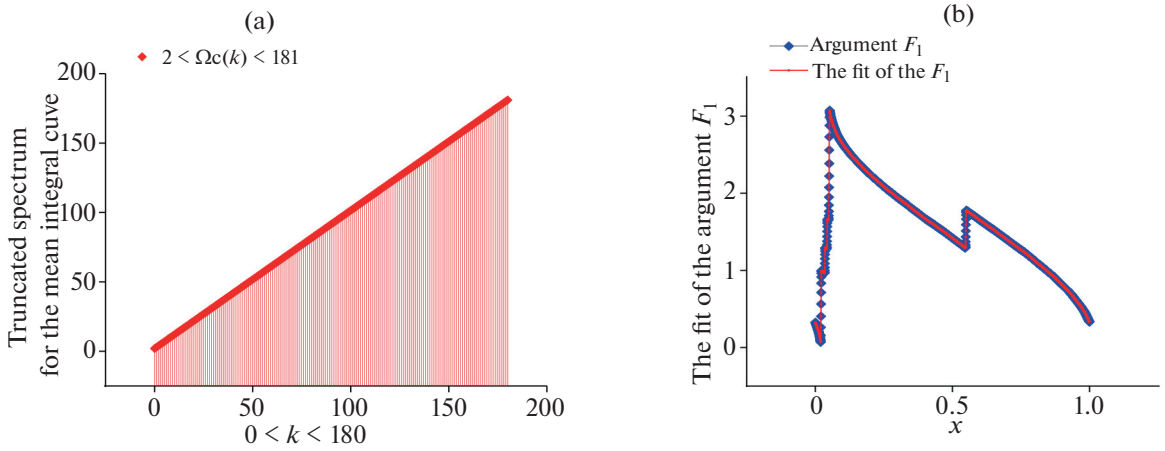

Fig. 7. In the left panel is shown a truncated spectrum located in the interval [2, 181]. In the right panel, the solid blue line shows the approximating function $Yft(t)$ for the function $F_1(t)$.

The approximate fitting function of the original signal is determined by the expression

$$\mathrm{Ex}(t) = a\cos\left(Yft(t)\right) + b,$$

where the scaling parameters a and b are found as the slope and intercept values, respectively, from the central Fig. 6b. In the same way, the random curves shown in Figure 2b can be approximated. Let us list the main ones (see Figs. 7–10).

The truncated spectrum in Fig. 7a is sufficient to provide an approximation with a relative error (defined by expression (4)) of less than 1%. The exact values of the relative error are presented in Table 1.

The solid straight line shown in Fig. 8b corresponds to the SRA for the ordered phases. It is easy to see that it is near in appearance to a straight line segment. This, once again, demonstrates that the phase distribution is almost uniform.

The truncated spectrum in Fig. 9a is sufficient to provide an approximation with a relative error (defined by expression (4)) of less than 1%. The exact values of the relative error are presented in Table 1.

The solid straight line that is shown in Fig. 10(b) corresponds to the SRA for the ordered phases. It can be seen that it is close in appearance to a straight line segment. This also confirms that the phase distribution is nearly uniform.

We consider the obtained values informative enough to confirm the effectiveness of the modified Fourier transform.

4. RESULTS AND DISCUSSION

The proposed modification of the traditional Fourier transform provides new possibilities for the approximation of a wide range of random functions. It can be argued that any given function has its own AFR, which is located inside the argument of the cosine (see expressions (2) and (3)) and gives, in fact, the true spectrum for signals with frequency-phase modulation and the second spectrum for amplitude-

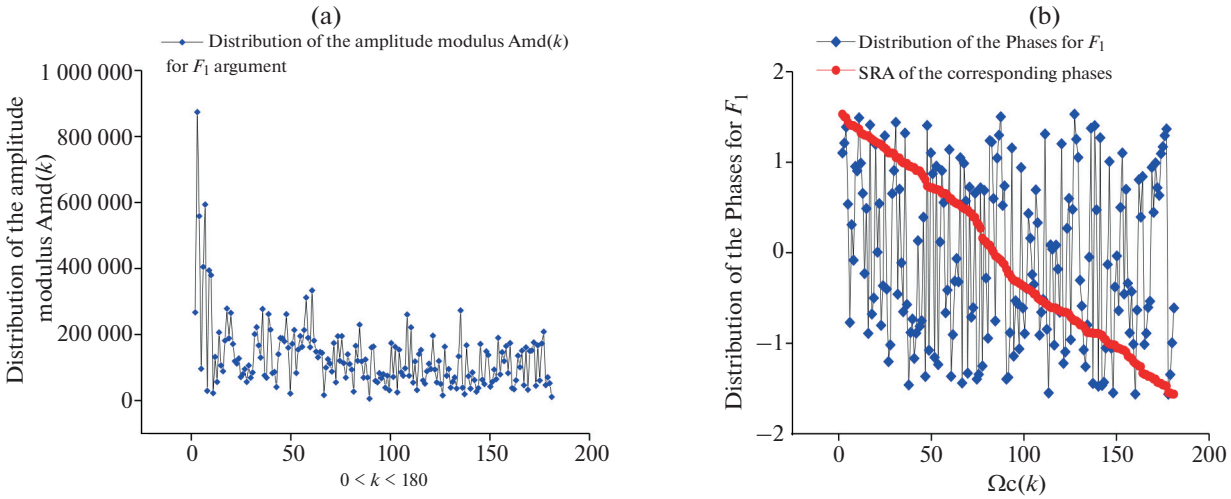

Fig. 8. The amplitude modules are shown in the panel, $\mathrm{Amd}_k = \sqrt{\mathrm{Ac}_k^2 + \mathrm{As}_k^2}$, and in the right is the phase distribution $\mathrm{Phase}_k = \tan^{-1}(\mathrm{As}_k / \mathrm{Ac}_k)$ for argument $F_1(t)$.

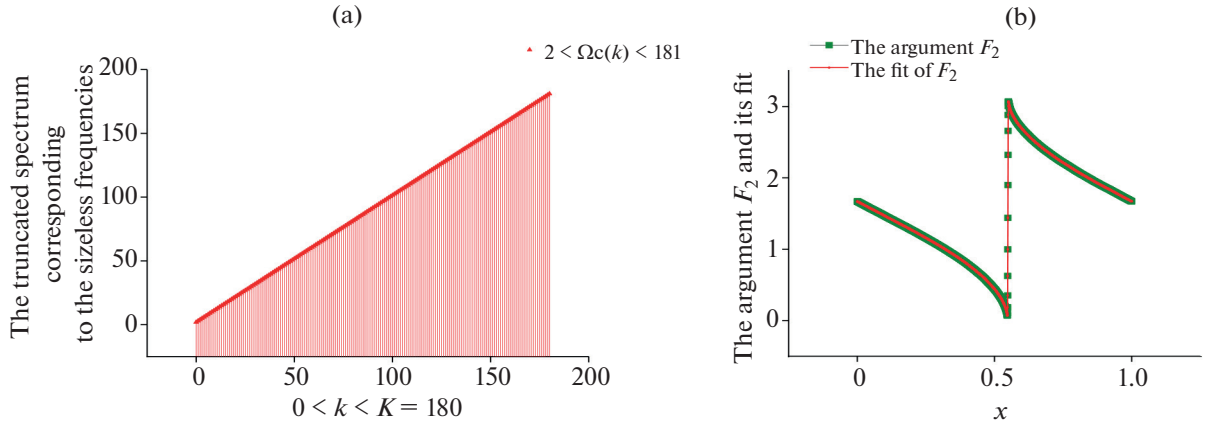

Fig. 9. In the left panel is shown a truncated spectrum located in the interval [2, 181]. In the right panel, the solid red line shows the approximating function *Yft*(*t*) for the function $F_2(t)$.

modulated signals. Indeed, if a random signal has the following structure:

$$\mathrm{Sg}(t) = A(t)\cos(Fr(t)) \to a\cos(F(t)) + b,$$

then the right side of the random signal Sg(*t*) includes all three types of possible modulations (amplitude, frequency, and phase). The transformation used in this work is fully applicable for two types of modulation (frequency and phase) as an exact transformation, and for amplitude modulation it can be considered as an approximate one. The AFR calculated for the function *F*(*t*) can be considered a useful secondary spectrum in the analysis and approximation of various random signals with amplitude modulation. If there is no amplitude modulation, then dependence (2) is unique and accurate. Formula (2) allows the following generalization (if Sg(*t*) is represented as a single mode)

$$\mathrm{Sg}(t) = A\cos(F(t)) + B\sin(F(t)),$$

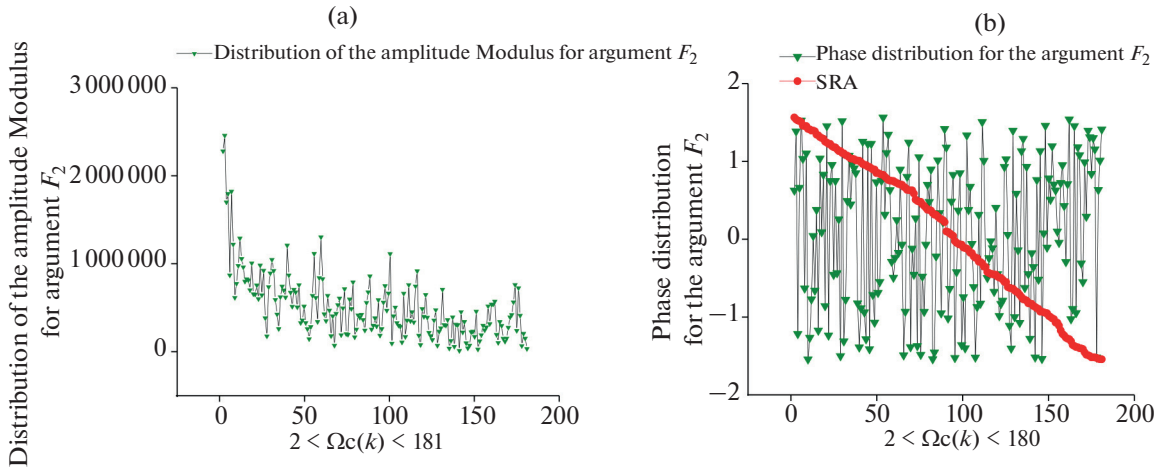

Fig. 10. The amplitude module is shown in the left panel, $\mathrm{Amd}_k = \sqrt{\mathrm{Ac}_k^2 + \mathrm{As}_k^2}$, and in the right is the phase distribution $\mathrm{Phase}_k = \tan^{-1}(\mathrm{As}_k / \mathrm{Ac}_k)$ for argument $F_2(t)$.

where constants A and B are assumed to be known. From here we can find the argument $F(t)$

$$F(t) = \cos^{-1}\left(\frac{\mathrm{Sg}(t)}{\sqrt{A^2 + B^2}}\right) + \tan^{-1}\left(\frac{A}{B}\right). \qquad (5)$$

Thus, expression (5) generalizes the previous expressions and expands the scope of application of the proposed modified Fourier transform.

Let us highlight the main results obtained.

1. For the random function $\mathrm{Sg}(t)$, a purely periodic function $F(t)$ is found.

2. This function $F(t)$ is related nonlinearly to the original random signal.

3. The proposed approach solves the problem of the approximation of a wide class of signals with frequency-phase modulation.

4. Due to this, the wide application of this modification of the Fourier transform will be useful, in particular, for describing the responses of various complex systems, such as technical, financial, medical, etc., when a simple model is missing.

ABBREVIATIONS AND NOTATION

AFR	amplitude-frequency response
NOCFASS	non-orthogonal combined Fourier analysis of the smoothed signals
SRA	sequence of the range amplitudes

FUNDING

The work was carried out using funds from a subsidy allocated to Kazan Federal University for the implementation of a state assignment in the field of scientific activity, project No. FZSM-2024-0004.

CONFLICT OF INTEREST

The authors of this work declare that they have no conflicts of interest.

REFERENCES

1. Mertins, A., *Signal Analysis: Wavelets, Filter Banks, Time-Frequency Transforms and Applications*, Chichester: Wiley, 1999.
2. Arecchi, F.T., Meucci, R., Puccioni, G., and Tredicce, J., Experimental evidence of subharmonic bifurcations, multistability, and turbulence in a *Q*-switched gas laser, *Phys. Rev. Lett.*, 1982, vol. 49, no. 17, pp. 1217–1220. https://doi.org/10.1103/PhysRevLett.49.1217
3. Chen, J.H., Chau, K.T., Chan, C.C., and Jiang, Q., Subharmonics and chaos in switched reluctance motor drives, *IEEE Trans. Energy Convers.*, 2002, vol. 17, no. 1, pp. 73–78. https://doi.org/10.1109/60.986440
4. Lauterborn, W. and Cramer, E., Subharmonic route to chaos observed in acoustics, *Phys. Rev. Lett.*, 1981, vol. 47, no. 20, pp. 1445–1448. https://doi.org/10.1103/physrevlett.47.1445
5. Wilden, I., Herzel, H., Peters, G., and Tembrock, G., Subharmonics, biphonation, and deterministic chaos in mammal vocalization, *Bioacoustics*, 1998, vol. 9, no. 3, pp. 171–196. https://doi.org/10.1080/09524622.1998.9753394
6. Cohen, L., *Time-Frequency Analysis*, Englewood, NJ: Prentice Hall, 1995.
7. Almeida, L.B., The fractional Fourier transform and time-frequency representations, *IEEE Trans. Signal Process.*, 1994, vol. 42, no. 11, pp. 3084–3091. https://doi.org/10.1109/78.330368
8. Sejdić, E., Djurović, I., and Stanković, L., Fractional Fourier transform as a signal processing tool: An overview of recent developments, *Signal Process.*, 2011, vol. 91, no. 6, pp. 1351–1369. https://doi.org/10.1016/j.sigpro.2010.10.008

9. Su, X., Tao, R., and Kang, X., Analysis and comparison of discrete fractional Fourier transforms, *Signal Process.*, 2019, vol. 160, pp. 284–298. https://doi.org/10.1016/j.sigpro.2019.01.019

10. Portnoff, M., Time-frequency representation of digital signals and systems based on short-time Fourier analysis, *IEEE Trans. Acoust., Speech, Signal Process.*, 1980, vol. 28, no. 1, pp. 55–69. https://doi.org/10.1109/tassp.1980.1163359

11. Qian, Sh. and Chen, D., Joint time-frequency analysis, *IEEE Signal Process. Mag.*, 1999, vol. 16, no. 2, pp. 52–67. https://doi.org/10.1109/79.752051

12. Li, M., Liu, Yo., Zhi, Sh., Wang, T., and Chu, F., Short-time Fourier transform using odd symmetric window function, *Journal of Dynamics, Monitoring and Diagnostics*, 2022, vol. 1, no. 1, pp. 37–45. https://doi.org/10.37965/jdmd.v2i2.39

13. Hlubina, P., Luňáček, J., Ciprian, D., and Chlebus, R., Windowed Fourier transform applied in the wavelength domain to process the spectral interference signals, *Opt. Commun.*, 2008, vol. 281, no. 9, pp. 2349–2354. https://doi.org/10.1016/j.optcom.2007.12.028

14. Kemao, Q., Windowed Fourier transform for fringe pattern analysis, *Appl. Opt.*, 2004, vol. 43, no. 13, pp. 2695–2702. https://doi.org/10.1364/ao.43.002695

15. Qian, S. and Chen, D., Discrete Gabor transform, *IEEE Trans. Signal Process.*, 1993, vol. 41, no. 7, pp. 2429–2438. https://doi.org/10.1109/78.224251

16. Yao, J., Krolak, P., and Steele, C., The generalized Gabor transform, *IEEE Trans. Image Process.*, 1995, vol. 4, no. 7, pp. 978–988. https://doi.org/10.1109/83.392338

17. Zhao, Zh., Tao, R., Li, G., and Wang, Yu., Clustered fractional Gabor transform, *Signal Process.*, 2020, vol. 166, p. 107240. https://doi.org/10.1016/j.sigpro.2019.107240

18. Mallat, S., *A Wavelet Tour of Signal Processing*, Burlington, MA: Academic, 1999, 3rd ed. https://doi.org/10.1016/B978-012466606-1/50008-8

19. Yan, R., Gao, R.X., and Chen, X., Wavelets for fault diagnosis of rotary machines: A review with applications, *Signal Process.*, 2014, vol. 96, pp. 1–15. https://doi.org/10.1016/j.sigpro.2013.04.015

20. Kumar, A., Wavelet signal processing: A review for recent applications, *International Journal of Engineering and Techniques*, 2020, vol. 6, no. 6, pp. 1–7. https://doi.org/10.29126/23951303/ijet-v6i6p7

21. Peng, Z.K., Tse, P.W., and Chu, F.L., A comparison study of improved Hilbert–Huang transform and wavelet transform: Application to fault diagnosis for rolling bearing, *Mech. Syst. Signal Process.*, 2005, vol. 19, no. 5, pp. 974–988. https://doi.org/10.1016/j.ymssp.2004.01.006

22. Zayed, A.I., Hilbert transform associated with the fractional Fourier transform, *IEEE Signal Process. Lett.*, 1998, vol. 5, no. 8, pp. 206–208. https://doi.org/10.1109/97.704973

23. Souza, U.B.D., Escola, J.P.L., and Brito, L.D.C., A survey on Hilbert–Huang transform: Evolution, challenges and solutions, *Digital Signal Process.*, 2021, vol. 120, no. 4, p. 103292. https://doi.org/10.1016/j.dsp.2021.103292

24. Bhattacharyya, A., Singh, L., and Pachori, R.B., Fourier–Bessel series expansion based empirical wavelet transform for analysis of non-stationary signals, *Digital Signal Process.*, 2018, vol. 78, pp. 185–196. https://doi.org/10.1016/j.dsp.2018.02.020

25. Chaudhary, P.K., Gupta, V., and Pachori, R.B., Fourier–Bessel representation for signal processing: A review, *Digital Signal Process.*, 2023, vol. 135, p. 103938. https://doi.org/10.1016/j.dsp.2023.103938

26. Huang, N.E., Shen, Zh., Long, S.R., Wu, M.C., Shih, H.H., Zheng, Q., Yen, N.-C., Tung, Ch.Ch., and Liu, H.H., The empirical mode decomposition and the Hilbert spectrum for nonlinear and non-stationary time series analysis, *Proc. R. Soc. London, Ser. A*, 1998, vol. 454, no. 1971, pp. 903–995. https://doi.org/10.1098/rspa.1998.0193

27. Wu, Zh. and Huang, N.E., Ensemble empirical mode decomposition: A noise-assisted data analysis method, *Advances in Adaptive Data Analysis*, 2009, vol. 1, no. 1, pp. 1–41. https://doi.org/10.1142/s1793536909000047

28. Nigmatullin, R.R., Alexandrov, V.S., Agarwal, P., Jain, Sh., and Ozdemir, N., Description of multi-periodic signals generated by complex systems: NOCFASS—New possibilities of the Fourier analysis, *Numer. Algebra, Control Optim.*, 2024, vol. 14, no. 1, pp. 1–19. https://doi.org/10.3934/naco.2022008

SPELL: 1. OK